3-2009

Oogenesis Defects in a Mutant Mouse Model of Oculodentodigital Dysplasia

Dan Tong
University of Western Ontario

Deanne Colley
University of Western Ontario

Renee Thoo
University of Western Ontario

Tony Y. Li
University of Western Ontario

Isabelle Plante
University of Western Ontario, iplante@uwo.ca

See next page for additional authors

Authors
Dan Tong, Deanne Colley, Renee Thoo, Tony Y. Li, Isabelle Plante, Dale W. Laird, Donglin Bai, and Gerald M. Kidder

Oogenesis defects in a mutant mouse model of oculodentodigital dysplasia

Dan Tong[1-3], Deanne Colley[1-3], Renee Thoo[1], Tony Y. Li[1-3], Isabelle Plante[5], Dale W. Laird[1,5], Donglin Bai[1], Gerald M. Kidder[1-4]

[1]Departments of Physiology and Pharmacology, [2]Obstetrics and Gynaecology, [3]Paediatrics, and [5]Anatomy and Cell Biology, Schulich School of Medicine and Dentistry, The University of Western Ontario, London, ON and [4]Children's Health Research Institute, 800 Commissioners Road East, London, ON

Address for correspondence:

Dr. Gerald M. Kidder
Department of Physiology and Pharmacology
Schulich School of Medicine and Dentistry
The University of Western Ontario
London, ON N6A 5C1
tel: 519-661-3132
fax: 519-850-2562
gerald.kidder@schulich.uwo.ca

Running title: Effects of $Cx43^{G60S}$ mutant on oogenesis

Summary

The essential role of connexin43 (Cx43) during oogenesis has been demonstrated by the severe germ cell deficiency and arrested folliculogenesis observed in Cx43 knockout mice. Recently, another mutant mouse strain became available (*Gja1*^{Jrt}/+) that carries the dominant loss-of-function Cx43 mutation, Cx43^{G60S}. *Gja1*^{Jrt}/+ mice display features of the human disease, oculodentodigital dysplasia (ODDD), caused by mutations in the *GJA1* gene. We have used this new mutant strain to study how a disease-linked Cx43 mutant affects oogenesis. We found that female mutant mice are subfertile with significantly reduced mating success and small litters. The phosphorylated species of the Cx43 protein are reduced in the mutant ovaries in association with impaired trafficking and assembly of gap junctions in the membranes of granulosa cells, confirming that the mutant protein acts dominantly on its wild-type counterpart. Correspondingly, although starting with normal abundance of germ cells, ovaries of the mutant mice contain significantly fewer pre-ovulatory follicles and do not respond to superovulation by gonadotropins, which is at least partially due to reduced proliferation and increased apoptosis of granulosa cells. We conclude that the *Gja1*^{Jrt} mutation has a dominant negative effect on Cx43 function in the ovary, rendering the females subfertile. Given these findings, closer examination of reproductive function in ODDD human females is warranted.

Key words: Connexin43, Gap junction, Granulosa cell, Folliculogenesis, ODDD, Primordial germ cell, Oocyte maturation, Fertilization

Introduction

Connexins are the protein subunits of gap junction channels, which enable neighboring cells to exchange small signaling molecules (less than ~1 kDa) and to synchronize electrical activities. Six identical or different connexins hexamerize to form a homomeric or heteromeric connexon (hemichannel), respectively. Two connexons (hemichannels) from adjacent cells dock with each other to form an intercellular gap junction channel (reviewed by Laird, 2006). So far, 20 and 21 connexin genes are found in the mouse and the human genomes, respectively, which have distinct, but overlapping patterns of expression (Laird, 2006).

The ovarian follicle provides a good example of a multicellular unit that exhibits expression of multiple connexins and is considered to be reliant upon gap junctional intercellular communication (GJIC) for proper development (reviewed by Kidder, 2005). As the most abundant connexin in the ovary, Cx43 is continuously expressed in the mouse fetal ovary from the onset of ovarian differentiation (Perez-Armendariz et al., 2003). After birth, Cx43 forms numerous, large gap junctions among granulosa cells in primordial, primary, secondary and antral follicles with the expression level increasing in parallel with follicle development (reviewed by Granot & Dekel, 2002). The essential role of Cx43 during oogenesis and folliculogenesis has been clearly demonstrated by the Cx43 knockout mice (*Gja1*$^{-/-}$). Offspring (both male and female) homozygous for the null mutation have very few primordial germ cells (PGCs) (Juneja et al., 1999). The marked loss of PGCs is at least partially due to increased apoptosis associated with abnormal P53 activation in the germ cells, demonstrating that Cx43 is required for PGC survival in the genital ridges (Francis and Lo, 2006). However, the gonads of Cx43 null

fetuses do contain germ cells, about 10% of the normal number (Juneja et al., 1999). Due to the neonatal death of Cx43 null mice, late fetal ovaries were grafted into the kidney capsule of ovariectomized adult mice to allow postnatal follicular development. In contrast to the full range of follicles from primordial through large preovulatory follicles observed in grafted wildtype ovaries, folliculogenesis in mutant ovaries of the C57BL/6 strain did not proceed beyond the primary unilaminar stage (Ackert et al., 2001). Further study demonstrated that intercellular coupling among granulosa cells was totally abolished in Cx43 null mice, indicating a requirement for coupling among granulosa cells via Cx43 channels to sustain granulosa cell proliferation (Gittens et al., 2003; Gittens et al., 2005; Tong et al., 2006). Failure of the Cx43 null follicles to develop multiple layers of granulosa cells was correlated with reduced growth of the oocytes, which were morphologically abnormal, meiotically incompetent and could not be fertilized (Ackert et al., 2001).

Oculodentodigital dysplasia (ODDD) is a rare human autosomal dominant disorder caused by mutations in the *GJA1* gene encoding Cx43. Common symptoms include syndactyly of hands and feet, enamel hypoplasia, craniofacial abnormalities, ophthalmic defects and occasionally heart and neurological dysfunction (Loddenkemper et al., 2002; Paznekas et al., 2003). More than 39 different ODDD-causing mutations in the gene encoding Cx43 have been identified so far (reviewed by Laird, 2006). In vitro studies of the ODDD-linked Cx43 mutants have shown that most mutants will assemble into gap junction plaque-like structures at the cell surface to varying degrees, however, all provide severely reduced gap junctional intercellular communication as compared to wild-type Cx43. Furthermore, when co-expressed with

wild-type Cx43, the mutants often act in dominant-negative fashion (Roscoe et al., 2005; Shibayama et al., 2005; McLachlan et al., 2005).

In 2005, a mouse model of ODDD became available when an N-ethyl-N-nitrosourea mutagenesis screen resulted in the generation of a mouse that exhibits many classic symptoms of ODDD including syndactyly, enamel hypoplasia, and craniofacial bone anomalies (Flenniken et al., 2005). This mouse carries a G60S point mutation (product of the *Gja1*^{Jrt} allele) in the first extracellular loop of Cx43, one residue removed from the P59H mutation identified in human ODDD patients (Vasconcellos et al., 2005). Our previous work demonstrated that the granulosa cells isolated from these mice (*Gja1*^{Jrt}/+) exhibit either very weak coupling (10-20% vs wild-type) or a complete lack of coupling, indicating that the G60S mutant dominantly inhibits the function of co-expressed wild-type Cx43 *in vivo* (Flenniken et al., 2005). Given the defects observed in Cx43 null ovaries, we hypothesized that Cx43^{G60S} affects oogenesis by inhibiting the function of wild-type Cx43 during germ cell migration and folliculogenesis. To test this hypothesis, we compared fertility, germ cell numbers, and follicular development of *Gja1*^{Jrt}/+ females with their wild-type littermates. We found that the mutant mice are subfertile with reduced mating success and smaller litter size compared with wild-type siblings. Although they have normal germ cell numbers, ovaries of the mutant mice contain significantly fewer pre-ovulatory follicles and are impaired in their response to gonadotropins. This was associated with impaired phosphorylation of Cx43 protein and reduced GJIC among granulosa cells.

Results

Female Gja1^{Jrt}/+ mice have reduced fertility

After mating with wild-type males, the pregnancy rate of female *Gja1*^{Jrt}/+ mice (23.5%, n=34 matings) was much lower than their wild-type littermates (83.9%, n=31) (Fig. 1A.). Furthermore, when *Gja1*^{Jrt}/+ females were mated with wild-type males, their mean litter size (3.0 ± 0.2, n = 46 litters) was significantly smaller ($P < 0.001$) compared with those resulting from mating between wild-type females and wild-type males (7.9 ± 0.3, n = 53). Surprisingly, litter sizes were normal (7.0 ± 0.2, n = 172; $P > 0.05$ compared with wild type) if only the males were carrying the mutation (Fig. 1B.), indicating that the mutation selectively affects female fertility. In addition, litter sizes were further reduced given the fact that only around 16% of the pups survived beyond postnatal day 1 if the mother carried the mutation (Fig. 1C.), which was due at least partially to a co-existent lactation problem described elsewhere (Plante & Laird, 2008).

Gja1^{Jrt}/+ ovaries contain normal numbers of germ cells

To determine whether the abundance of germ cells may be affected by the *Gja1*^{Jrt} mutation, we counted germ cell numbers in the postnatal day 1 ovaries using GCNA as a specific germ cell marker (Juneja et al., 1999). In contrast to the severe germ cell deficiency observed in *Gja1*$^{-/-}$ ovaries, there was no significant difference ($P = 0.71$) in germ cell numbers between *Gja1*^{Jrt}/+ females (n = 3639 ± 988) and their wild-type littermates (n = 4123 ± 227) (Fig. 2B). Three ovaries from 3 different mice were counted for each genotype. As shown in Figure 2A, germ cells in the ovaries of both genotypes showed similar peripheral distribution in the ovarian cortex, however, the numerous Cx43 gap junction “plaques” present in the somatic cells were barely

observed in the mutant ovaries.

Gja1^{Jrt}/+ ovaries contain fewer pre-ovulatory follicles and have reduced response to gonadotropins

Although starting with similar numbers of germ cells, ovaries of sexually mature *Gja1*^{Jrt}/+ females contain significantly fewer pre-ovulatory follicles at proestrus (Fig. 3B; $P < 0.05$ vs. wild-type littermates, two-way ANOVA and Bonferroni post hoc test, n = 4 ovaries from 4 mice). However, there was no significant difference in the distribution of earlier follicle stages (Fig. 3A; $P > 0.05$, Chi-square test, n = 3 ovaries from 3 mice for each group), indicating that the mutation mainly affected the final maturation of the follicles. Morphologically atretic follicles were rarely seen in ovaries of both groups. To test their response to gonadotropins, mice from both genotypes were primed with chorionic gonadotropin (eCG), a peptide hormone with follicle-stimulating hormone (FSH) activity in the mouse, and induced to ovulate with human chorionic gonadotropin (hCG) as a source of luteinizing hormone (LH) activity. Significantly fewer oocytes were collected from the oviducts of the *Gja1*^{Jrt}/+ females (19.6 ± 9.5, n = 5 mice vs. 60.0 ± 3.8, n = 4 mice from wild-type, unpaired t-test, $P < 0.01$), indicating that the response of the mutant mice to gonadotropins is reduced (Fig. 3C).

Oocytes from *Gja1*^{Jrt}/+ females are developmentally competent

To test the meiotic competence of the oocytes, cumulus-oocyte complexes were obtained from punctured antral follicles of females primed with eCG. After Hoechst nuclear staining, it was apparent that oocytes from the *Gja1*^{Jrt}/+ females are equally as

competent as wild-type oocytes in undergoing the first meiotic division to produce the first polar body (Table 1). Although fewer oocytes can be collected from the oviducts of *Gja1*^{Jrt}/+ females primed with eCG and hCG, these oocytes were able to develop to the two-cell stage at a frequency similar to wild-type after being fertilized (Fig. 3D; n = 50 wild-type and 20 mutant oocytes from 3 mice of each genotype). This indicates that female *Gja1*^{Jrt}/+ mice produce competent oocytes.

Phosphorylation and trafficking of Cx43 are aberrant in *Gja1*^{Jrt}/+ granulosa cells

Western blot analysis demonstrated that the abundance of total Cx43 protein in ovaries from *Gja1*^{Jrt}/+ mice is not significantly different from that of wild-type (1.5 ± 0.2 vs. 1.1 ± 0.1, $P > 0.05$; Fig. 4A). However, the phosphorylated P1 and P2 forms of Cx43 were significantly reduced in the mutant ovaries (1.3 ± 0.2 for wild-type vs. 0.7 ± 0.1 for *Gja1*^{Jrt}/+, $P < 0.01$, two-way ANOVA, n = 9 blots from 6 mice for each group), suggesting the mutation impairs phosphorylation of Cx43 in the ovaries. This result is slightly different from that of our previous study (Flenniken et al., 2005) showing that both total Cx43 level and its phosphorylated species are significantly downregulated in the mutant ovaries. This is probably due to different strain backgrounds and different ages of the mice used in the two studies. To further confirm this, ovary and heart from the same mice were loaded on gels for western blotting. As shown in Fig. 4A, the abundance of Cx43 in the heart is significantly reduced in terms of both total Cx43 and its phosphorylated species ($P < 0.001$ for both, two-way ANOVA, n = 3 blots from 3 mice for each group), which is consistent with previous studies (Flenniken et al., 2005; Manias et al., 2008). The consequence of aberrant phosphorylation on gap junction

formation in ovaries was evaluated by immunostaining. As shown in Fig. 4B, compared with wild-type controls, there was a marked reduction in accumulation of Cx43 at the junctional membrane, visualized as Cx43 gap junction "plaques" in the follicles. To further visualize the trafficking of Cx43 on a cellular level, we isolated granulosa cells from the ovaries of wild-type and *Gja1*^{Jrt}/+ mice and examined the Cx43 expression profile. Consistent with tissue immunostaining, very few gap junction plaques were evident in the *Gja1*^{Jrt}/+ granulosa cells, whereas a much larger population of Cx43 was localized to the Golgi apparatus, indicating that the *Gja1*^{Jrt} mutation affected the normal trafficking of Cx43 to the cell membrane (Fig. 4C).

Proliferation of granulosa cells is reduced in *Gja1*^{Jrt}/+ ovaries

The absence of Cx43 has been associated with reduced granulosa cell proliferation (Gittens et al., 2005). Therefore, we evaluated the effect of the *Gja1*^{Jrt} mutation on granulosa cell growth. As demonstrated by BrdU uptake assay, only 14.7 ± 3.1 % of granulosa cells isolated from *Gja1*^{Jrt}/+ ovaries took up BrdU after a four-hour incubation, compared with 26.5 ± 3.3 % of the wild-type granulosa cells ($P < 0.05$, t-test, n = 15 and 13 fields from 6 mice in wild-type and mutant groups, respectively). To further confirm this, we quantified the expression of the cell proliferation marker PCNA and found that PCNA expression is significantly reduced in the mutant (0.7 ± 0.1 vs. 1.0 ± 0.04 for wild-type, $P < 0.01$, t-test, n = 52 fields from 6 mice for each group).

Apoptosis rate is elevated in Gja1^{Jrt}/+ antral follicles

To determine whether the reduced proportion of mature follicles observed in the mutant

ovaries was also due to an elevated rate of apoptosis of granulosa cells, we used the TUNEL assay to fluorescently label fragmented DNA of apoptotic cells. *Gja1*^{Jrt}/+ and wild-type ovaries were examined in parallel. As shown in Fig. 6A, apoptotic granulosa cells were prominent in the early antral follicles of *Gja1*^{Jrt}/+ ovaries but infrequent in wild-type follicles. The fluorescent intensities of TUNEL staining in antral follicles are quantified in Fig. 6B (n = 14 wild-type follicles from 5 mice vs. n = 17 *Gja1*^{Jrt}/+ follicles from 5 mice, $P < 0.05$, unpaired t-test). It appears that granulosa cell apoptosis is significantly elevated in antral follicles of *Gja1*^{Jrt}/+ ovaries.

Oocyte-granulosa cell coupling and GDF9 expression are not altered in Gja1^{Jrt}/+ ovaries

Previous work had indicated that the gap junctions coupling the oocyte with surrounding granulosa cells are composed of Cx37 with little or no contribution from Cx43 (Veitch et al., 2004; reviewed by Kidder, 2005). To test whether the *Gja1*^{Jrt}/+ mutation might also affect oocyte-granulosa cell coupling, the gap junction channel-permeant fluorescent dye, Lucifer yellow, was injected into granulosa cell-enclosed oocytes. As shown in Fig. 7A, in both wild-type and *Gja1*^{Jrt}/+ follicles, injected dye passed from oocytes to surrounding granulosa cells (n = 10 for wild-type vs. n = 13 for *Gja1*^{Jrt}/+), indicating that oocyte-granulosa cell coupling is still intact in *Gja1*^{Jrt}/+ ovaries. There was no obvious difference between genotypes in the rate of dye passage. However, less extensive dye spreading among the granulosa cells was observed in the *Gja1*^{Jrt}/+ follicles, confirming that the *Gja1*^{Jrt}/+ mutation preferentially impairs coupling among the granulosa cells.

Previous work with the Cx43 null mutant line (*Gja1*-/-) had indicated an interaction between Cx43-mediated gap junctional communication and intra-ovarian paracrine signaling, with the mutant granulosa cells having reduced responsiveness to the oocyte-derived mitogen, GDF9 (Gittens et al., 2005). GDF9 expression, however, was not reduced. Likewise, the expression of GDF9 in the $Gja1^{Jrt}$/+ ovaries did not differ from that in wild-type littermates (0.20 ± 0.01 for wild-type, n = 6 vs. 0.23 ± 0.02 for $Gja1^{Jrt}$/+, n = 6, P > 0.05, unpaired t-test; Fig. 7B). Thus it is unlikely that the impaired oogenesis observed in $Gja1^{Jrt}$/+ ovaries is due to altered expression of GDF9.

Discussion

The essential role of Cx43 during oogenesis has been demonstrated by previous studies using Cx43 knockout mice in which the absence of Cx43 caused severe germ cell deficiency and arrested folliculogenesis (Juneja et al., 1999; Ackert et al., 2001). Germ cells are known to express Cx43 and are well coupled to surrounding cells during their development (Francis and Lo, 2006). Cx43 is also present at all stages of ovary development where it contributes to coupling between the somatic cells. Therefore, it is believed that the intercellular communication mediated by Cx43 gap junctions is critical for germ cell survival and ovarian folliculogenesis. However, the knockout mouse model does not mimic any human condition since complete loss of Cx43 is lethal (Reaume et al., 1995). The $Gja1^{Jrt}$/+ mice, which have a phenotype resembling the human disease ODDD, provided us with a good model to study how a disease-linked Cx43 mutation can affect oogenesis.

Several *in vitro* studies have demonstrated that ODDD-linked Cx43 mutations

exert dominant negative effects on wild-type Cx43, severely limiting Cx43 mediated intercellular communication (Laird, 2006). Our data indicate that the mutation causes aberrant Cx43 phosphorylation, demonstrated by marked reduction in the phosphorylated species P1 and P2 and increased amount of the P0 form in the ovaries. This is consistent with the immunostaining results showing that most of the Cx43 is retained in the intracellular compartment with very few gap junction plaques being visible in the junctional membranes. This finding indicates that the *Gja1*^{Jrt} mutation impairs normal trafficking and assembly of Cx43 gap junction channels in the granulosa cells, presumably through the oligomerization of mutant and wild-type connexins and the impaired assembly of the resulting complex. However, the detailed mechanism underlying this anomaly awaits further investigation. Hypophosphorylation and reduced junctional plaque formation are consistent with our previous work showing that granulosa cells isolated from *Gja1*^{Jrt}/+ mice are very weakly coupled (10-20% vs. wild-type) or exhibit a complete lack of coupling (Flenniken et al., 2005), indicating a dominant negative effect of the *Gja1*^{Jrt}/+ mutation. A similarly severe reduction of intercellular coupling has been observed in other cell types including osteoblasts, mammary epithelium, and cardiomyocytes from the same *Gja1*^{Jrt}/+ mice (McLachlan et al., 2008; Plante and Laird, 2008; Manias et al., 2008; see Table 2).

Given these findings, it is surprising that germ cell abundance was not affected in the *Gja1*^{Jrt}/+ mice. It is known that Cx43 is expressed in germ cells and plays an essential role in maintaining their survival, since increased germ cell apoptosis was observed in Cx43 null genital ridges starting from E 11.5 day (Francis and Lo, 2006). In the *Gja1*^{Jrt}/+ mice, it is possible that the residual low level of coupling found in mutant

granulosa cells is also present in migrating primordial germ cells and is sufficient for maintaining the survival of those cells. Another possibility is that the role of Cx43 in migrating germ cells does not involve gap junctional intercellular communication (GJIC), but is based on other functions of the connexin molecule (reviewed by Jiang and Gu, 2005). For example, it was demonstrated that Cx43 can interact with the growth factor NOV/CCN3 (nephroblastoma overexpression gene/connective-tissue growth factor) through its C-terminal (CT) domain, regulating cell proliferation (Fu et al., 2004; Gellhaus et al., 2004). Since the mutated Cx43 still has an intact CT, functions of the molecule that depend on binding to other cellular proteins via this segment may well remain intact. Indeed, it was recently reported that some ODDD-linked mutations, including G21R, G138R and G60S, still interact with caveolin whereas fs260, a frameshift mutation in which the C-terminal region is altered and truncated, did not co-immunoprecipitate with caveolin (Langlois et al., 2008). Therefore, it will be interesting to examine oogenesis in a mouse model carrying the ODDD fs260 mutation. The same explanation may also apply to the presence of follicles of all developmental stages in *Gja1*^{Jrt}/+ ovaries, in contrast to the arrested folliculogenesis observed in Cx43 knockout females (Ackert et al., 2001).

In any case, *Gja1*^{Jrt}/+ females are subfertile with significantly reduced mating success and smaller litter size compared with their wild-type siblings. Although starting with normal numbers of germ cells, ovaries of the mutant mice contain significantly fewer pre-ovulatory follicles and have reduced response to gonadotropins, which can at least partially explain the observed reduction of fertility. Like Cx43 null granulosa cells (Gittens et al., 2005), granulosa cells isolated from *Gja1*^{Jrt}/+ females

have a reduced proliferation rate. However, unlike Cx43 null granulosa cells, granulosa cells in *Gja1*^{Jrt}/+ antral follicles demonstrated significantly higher apoptosis frequency. This difference is possibly associated with the additional dominant negative effect of the mutant Cx43 protein on wild-type Cx43 function in granulosa cells. Another possibility is that the role of Cx43 in preventing granulosa cells from undergoing apoptosis is follicle stage dependent, since few if any follicles develop to antral stages in Cx43 null ovaries (Ackert et al., 2001; Tong et al., 2006). This too must await further investigation. Together, these factors may collectively contribute to the reduced number of mature follicles observed in the *Gja1*^{Jrt}/+ ovaries. Previous work demonstrated that Cx43 is required for granulosa cells to fully respond to the oocyte-derived mitogen, GDF9 (Gittens et al., 2005) and another study showed that GDF9 protects granulosa cells from apoptosis and is required for the maintenance of FSH receptor expression (Orisaka et al., 2006). The present study confirmed that the expression of GDF9 is not altered in *Gja1*^{Jrt}/+ ovaries, the same as what was observed in *Gja1-/-* ovaries (Gittens et al., 2005). Therefore, the *Gja1*^{Jrt} mutation may affect the normal response of granulosa cells to endocrine and paracrine signals, thus restricting final maturation of the follicles.

Our finding that the *Gja1*^{Jrt} mutation preferentially affects coupling among the granulosa cells and leaves oocyte-cumulus cell coupling intact is consistent with the accumulated evidence that Cx43 is preferentially assembled into the gap junctions connecting granulosa cells whereas Cx37 forms the gap junctions connecting oocytes with granulosa cells (reviewed by Kidder, 2005). This view was supported recently by Gershon et al. (2008), who studied conditional knockout mice in which Cx43 was

depleted from oocytes by using the oocyte-specific *Zp3* promoter to drive CRE recombinase expression in growing oocytes carrying floxed *Gja1* alleles (there was also some reduction of Cx43 expression in the granulosa cells). Gershon et al. reported that the Cx43-deficient oocytes retained gap junctional coupling with the granulosa cells, underwent meiotic maturation in response to LH, and developed normally to the blastocyst stage after fertilization. However, the females producing Cx43-deficient oocytes exhibited a decrease in litter size, an effect that was traced to a reduction in the ability of their blastocysts to implant in the uterus. Thus it remains possible that Cx43 deficiency in developing oocytes has an impact on oocyte/embryo developmental competence that does not manifest itself until implantation. Further experiments will be needed to explore the possibility that implantation failure contributes to the reduced litter sizes of $Gja1^{Jrt}$/+ females.

It is of interest to compare the $Gja1^{Jrt}$/+ phenotype with those of the other two mutant mouse models generated to date that carry human *GJA1* mutations: G138R and I130T (Kalcheva et al., 2007; Dobrowolski et al., 2008). Those mutants demonstrated overall ODDD-like phenotypes similar to the $Gja1^{Jrt}$/+ mice (summarized in Table 2). Studies of G138R and I130T mice have so far focused on the heart, where the same negative effects on Cx43 expression level, phosphorylation state, subcellular localization, and function in cardiomyocytes found in G60S mice (Flenniken et al., 2005; Manias et al., 2008) were reported. However, the described cardiac contraction waves of the three mutant strains were not identical; the differences will need to be examined more carefully within a single laboratory to confirm that they represent different effects of the three mutant alleles. A reduction in litter size was reported for

I130T and G138R females, but in both cases it was attributed to prenatal death; ovulation rate was not investigated (Kalcheva et al., 2007; Dobrowolski et al., 2008). It will be important to investigate whether defects in oogenesis similar to those of G60S females are also present in the I130T and G138R mutants.

Finally, we note that phenotypic descriptions of ODDD patients to date have not included the reproductive system, which has presumably not been investigated since neither men nor women with the ODDD syndrome have been reported to be infertile. The reduced fertility observed in *Gja1*^{Jrt}/+ female mice raises a concern that some human ODDD females may have unrecognized reproductive deficiencies related to *GJA1* mutations. Given this uncertainty and the prominent expression of Cx43 in human ovarian follicles (Wang et al., 2008), we believe that further clinical investigations of ODDD females are warranted.

Materials and Methods

Mouse breeding and genotyping

All animal experiments were approved by the Animal Use Subcommittee of the University Council on Animal Care at the University of Western Ontario. The *Gja1*^{Jrt}/+ mice were generated at the Centre for Modeling Human Disease, University of Toronto, and were kindly provided by Dr. Janet Rossant. The original mice were on a mixed C57BL/6J and C3H/HeJ background (Flenniken et al., 2005) and were backcrossed to C57BL/6J for up to 4 generations. Genotypes were determined by polymerase chain reaction (PCR) as previously described (Flenniken et al., 2005).

Fertility testing

Mice were housed under controlled lighting (12 h light, 12 h dark) and temperature (21–24 °C) conditions. To evaluate the fertility of mice with different genotypes, three mating groups were set up separately: wild-type male with wild-type female, *Gja1*^{Jrt}/+ male with wild-type female, wild-type male with *Gja1*^{Jrt}/+ female. All of the mice were sexually mature, at least 6 weeks old. One male and one female were housed together for up to 7 days for mating. Offspring were counted on postnatal day 1, including both living and identifiable dead pups. The survival rate was calculated by comparing pup numbers on postnatal days 1 and 7.

Superovulation

To test the ability to ovulate in response to gonadotropins, 3- to 4- week-old females were injected intraperitoneally with 5 IU equine chorionic gonadotropin (eCG) (Sigma-Aldrich, Canada) around 6 pm followed 48 hours later with 5 IU of human chorionic gonadotrophin (hCG) (Sigma-Aldrich, Canada). The females were killed 14 to 15 hours later by cervical dislocation following CO_2 anesthesia. The cumulus-oocyte-complexes (COCs) were collected from the oviductal ampullae and counted.

In vitro oocyte maturation

Female mice (3 to 4 weeks old) were killed 24 hours after eCG (5 IU) injection. Ovaries were removed and placed in Waymouth's MB 752/1 medium plus 5% FBS and 0.23 mM pyruvic acid (sodium salt; Sigma-Aldrich). Follicles were pierced with 25-gauge needles to liberate cumulus-oocyte complexes. Oocytes enclosed by a complete layer of

cumulus cells were washed through culture medium and transferred to a 35 mm Petri dish containing 3 ng/ml FSH (Puregon 100 i.u. follitropin ß; Organon Canada, Scarborough, ON) in 3 ml Waymouth's medium/5% FBS. Oocytes were matured for 18 hours in a 5% CO_2/5% O_2/90% N_2 (5/5/90) atmosphere at 37°C and stained with Hoechst 33342 (Molecular Probes, Eugene, OR) diluted 1:1000 in Waymouth's medium/5% FBS to evaluate oocyte maturation.

In vitro fertilization

Female mice (3 to 4 weeks old) were superovulated as described above. The cumulus-oocyte-complexes (COCs) were collected from the oviductal ampullae in pre-gassed HTF medium (Jackson Laboratory) with 4 mg/ml BSA, and transferred to 500 µl droplets of HTF/BSA under mineral oil (Sigma-Aldrich) containing approximately 2 x 10^5 sperm/ml. Sperm were collected from the cauda epididymi of mice 3-5 months of age. Inseminated oocytes were incubated for 4 hours at 37°C in a 5/5/90 atmosphere. They were then washed through three dishes of HTF/BSA and cultured for 24 hours in 1 ml HTF/BSA in four-well plates (Nunc) in 5/5/90 atmosphere at 37°C to yield two-cell stage embryos.

Ovarian histology and follicle counts

Ovaries were collected from 6-8 week old females to determine follicle distribution. Ovaries were fixed in Bouin's solution and embedded in paraffin and sectioned serially at a thickness of 5 µm. For histological examination, sections were deparaffinized in xylene and rehydrated in graduated ethanol solutions followed by staining with

hematoxylin and eosin. Follicles were classified as primary (a single layer of cuboidal granulosa cells), secondary (multiple layers of granulosa cells but lacking any sign of an antral cavity), early antral (with one or more small fluid-filled cavities) and late antral (having a single large cavity with the oocyte against one side of the follicle). Care was taken that only follicles sectioned through the nucleus of the oocyte were counted. For early stage (primary and secondary) follicle counts, 3-4 representative sections from each ovary were examined. For antral (early and late) follicle counts, ovaries were collected from mice selected at proestrus based on vaginal smears (Fox & Laird, 1970), and all sections from each ovary were examined. One ovary from each mouse was counted with 3-5 ovaries from each genotype being examined.

Granulosa cell culture

Follicles were isolated and cultured as described previously (Tong et al., 2006). Briefly, the ovaries of 6 to 8 week old female mice were placed in culture in Waymouth MB 752/1 medium containing 10% FBS, 100 U/ml penicillin, and 100 μg/ml streptomycin (Invitrogen, Canada). Surrounding fat and connective tissue were removed by using fine 30-gauge needles. The ovaries were then digested in medium containing 2 mg/ml type I collagenase (Sigma-Aldrich, Canada) to facilitate follicle release. Follicles were liberated by repeated aspiration and expulsion with a 1 ml pipettor. Follicles were washed with culture medium and transferred to another dish where oocytes and granulosa cells were separated by treatment with trypsin-EDTA (0.05% trypsin, 0.53 mM EDTA tetrasodium salt, Invitrogen) for 5 min followed by centrifugation at 4,000 rpm for 5 min. The supernatant (containing oocytes) was removed and the granulosa

cells resuspended in culture medium. They were transferred to 12 mm glass coverslips then cultured at 37°C in 5% CO_2/95% air for less than 48 hours.

Immunofluorescent staining

Granulosa cells grown on glass coverslips were fixed with ice cold 80% methanol/20% acetone for 20 minutes before blocking with 2% bovine serum albumin (BSA, Sigma-Aldrich, Canada) in PBS for 1 hour. Cx43 was detected using a rabbit polyclonal antibody (1:500) (Sigma-Aldrich, Canada). The Golgi apparatus was labeled with a mouse antibody towards a resident protein, GM130 (1:100, BD Transduction Laboratories, Mississauga, ON). Appropriate Alex594 or Alex488 conjugated anti-mouse and anti-rabbit secondary antibodies (Molecular Probes) were used at a 1:200 dilution. Nuclei were labeled with Hoechst 33342 (1:1000 dilution; Molecular Probes). Slides were imaged on a Zeiss (Thornwood, NY) LSM 510 META confocal microscope.

For germ cell counting, ovaries were collected from postnatal day 1 female littermates and fixed, embedded and sectioned as described above. Ovary sections were deparaffinized and washed 3 times with phosphate-buffered saline (PBS) before immunolabeling. Germ cell nuclear antigen (GCNA), a specific marker for germ cells, was detected with a rat anti-GCNA antibody without dilution (a gift from Dr. George Enders, University of Kansas Medical Center) and Texas Red conjugated anti-rat secondary antibody was used at 1:200 dilution (Molecular Probes). For determining germ cell numbers, GCNA positive cells were counted on consecutive sections for each ovary. Care was taken that only cells sectioned through the largest diameter of the

nucleus were counted. Ovary sections from 6-8 week old females were also immunolabeled with Cx43 antibody as described above.

Proliferation assays

Granulosa cells were grown on glass coverslips at 50-70% confluency. For bromodeoxyuridine (BrdU) uptake assay, BrdU (Sigma-Aldrich, Canada) was added into the culture medium to reach a final concentration of 10 μM. The cells were then incubated for 4 hours at 37°C in 5% CO_2/95% air. They were washed three times with PBS before being fixed with ice cold 80% methanol/20% acetone for 20 minutes. Following incubation with 2 M HCl for 20 minutes to denature DNA, granulosa cells were immunolabeled as described above. BrdU detection was carried out using a mouse anti-BrdU antibody (Sigma-Aldrich, Canada, 1:100) and Texas Red conjugated anti-mouse secondary antibody (1:200). Nuclei were labeled with Hoechst 33342 (1:1000). Cell counts were expressed as the percentage of cells positive for BrdU staining relative to the total number of cells in view, counted after Hoechst staining. The proliferation rate of granulosa cells was also evaluated by immunostaining with mouse anti-proliferating cell nuclear antigen (PCNA) antibody (1: 200, Sigma-Aldrich, Canada) and Texas Red conjugated anti-mouse secondary antibody (1:200). The densities of the PCNA signals were quantified using Zeiss LSM software (Thornwood, NY). To minimize variation between experiments, each measurement was normalized to one of the wild-type granulosa cell readings from the same experiment.

Apoptosis assay

Ovary sections were stained for apoptotic cells by incorporating fluorescein-12-dUTP at the 3'-OH ends of fragmented DNA using the TUNEL (TdT-mediated dUTP Nick-End Labeling) assay kit (Promega, Madison, WI) according to the manufacturer's instructions. Sections treated with DNase (1 mg/ml, 10 min) (Sigma-Aldrich, Canada) were used for positive control. To quantify the TUNEL staining in antral follicles, the average pixel intensity for the area of antral follicles was determined using ImageJ 1.38x software (National Institutes of Health, USA).

Western blot analysis

Ovaries or hearts were homogenized in single-detergent lysis buffer supplemented with 1 mM NaF, 1 mM Na_3VO_4 and protease inhibitor cocktail (1 tablet per 10 ml buffer) (Sigma-Aldrich, Canada). Protein concentrations were determined using bicinchonic acid (BCA) assay (Pierce Biotechnology Inc., Rockford IL). 50 µg of protein was separated by electrophoresis on 12% SDS-PAGE gels and transferred to a nitrocellulose membrane. The membrane was incubated with either a rabbit anti-Cx43 antibody (1:1,000, Sigma-Aldrich, Canada), a goat anti-GDF9 antibody (c-20) (1:400, Santa Cruz, CA) or a mouse anti-GAPDH antibody (1:10,000, Chemicon, Temecula, CA) overnight at 4°C. Following three washes with Tris-buffered saline containing Tween 20 (five minutes each at room temperature), infrared fluorescent-labeled secondary antibodies (IRDye 800 anti-rabbit, Rockland Immunochemicals, Gilbertsville, PA; Alexa-680 anti-mouse, Molecular Probes, Eugene, OR) were incubated at room temperature for 1 h and immunoblots were processed and quantified using the Odyssey infrared-imaging system (Licor).

Oocyte microinjection

Ovarian follicles were isolated as described above and transferred to 12 mm glass coverslips then cultured at 37°C in 5% CO_2 / 95% air for 24 hours. The oocytes were impaled for 10 minutes with a 1 mm thin-wall glass capillary (World Precision Instruments, Sarasota, FL), tip diameter 1 μm, which was backfilled with 5% Lucifer yellow (Molecular Probes, Eugene, OR) in ddH_2O via capillary action. Dye was injected using an Eppendorf InjectMan NI 2 microinjection system and a Leica DMIRE2 inverted microscope with a 20x, 0.5 numerical aperture objective. Images were captured using a Hamamatsu C4742-95ER camera with Openlab software. Only those injections were recorded in which the dye filled the oocyte within 1 minute, as evidenced by bright fluorescence.

Data analysis and statistics

The data are expressed as mean ± s.e.m., with "n" denoting the number of independent experiments. Comparison of two groups was carried out using a two-tailed unpaired t-test, with a P value below 0.05 indicating significance. Comparison of more than two groups was carried out with one-way ANOVA followed by a Tukey test. Two-way ANOVA and Bonferroni test were used to compare two groups under different experimental conditions. Statistical significance is indicated in the graphs with a single asterisk (*) for $P < 0.05$, double for $P < 0.01$, and triple for $P < 0.001$.

Author Contributions

This work was a collaboration between the laboratories of D.B., G.M.K., and D.W.L. who jointly provided supervision and technical advice. D.T. performed most of the experiments and drafted the manuscript. D.C. contributed the data for Fig. 3A. R.T. contributed to the results of Fig. 2B and Fig. 5. T.Y.L. contributed the data for Fig. 7A. I.P. contributed data to Fig. 1C and part of Fig. 1A.

Acknowledgements

We thank Dr. Janet Rossant and the Centre for Modeling Human Disease for generously providing the *Gja1*^{Jrt}/+ mice. We are grateful to Kevin Barr for his expert advice, technical assistance, and management of the mouse colony. We thank Crystal Lounsbury for her assistance with management of the mouse colony and Dr. Hong-Xing Wang, Dr. Elizabeth McLachlan, and Janet Manias for their technical assistance. This work was funded by grants from the Canadian Institutes of Health Research (CIHR) to Donglin Bai, Gerald M. Kidder, and Dale W. Laird. Dan Tong was supported by a CIHR Canada Graduate Scholarship Doctoral Award.

References

Ackert, C. L., Gittens, J. E., O'Brien, M. J., Eppig, J. J. and Kidder, G. M. (2001). Intercellular communication via connexin43 gap junctions is required for ovarian folliculogenesis in the mouse. *Dev. Biol.* **233,** 258-270.

Dobrowolski, R., Sasse, P., Schrickel, J. W., Watkins, M., Kim, J. S., Rackauskas, M., Troatz, C., Ghanem, A., Tiemann, K., Degen, J. et al. (2008). The conditional

connexin43G138R mouse mutant represents a new model of hereditary oculodentodigital dysplasia in humans. *Hum. Mol. Genet.* **17,** 539-554.

Flenniken, A. M., Osborne, L. R., Anderson, N., Ciliberti, N., Fleming, C., Gittens, J. E., Gong, X. Q., Kelsey, L. B., Lounsbury, C., Moreno, L. et al. (2005). A Gja1 missense mutation in a mouse model of oculodentodigital dysplasia. *Development* **132,** 4375-4386.

Fox, R. and Laird, C. (1970). Sexual cycles. In *Reproduction and breeding techniques for laboratory animals* (ed. Hafez, E.S.E.), pp.107-122. Lee and Febiger, Philadelphia.

Francis, R. J. and Lo, C. W. (2006). Primordial germ cell deficiency in the connexin 43 knockout mouse arises from apoptosis associated with abnormal p53 activation. *Development* **133,** 3451-3460.

Fu, C. T., Bechberger, J. F., Ozog, M. A., Perbal, B. and Naus, C. C. (2004). CCN3 (NOV) interacts with connexin43 in C6 glioma cells: Possible mechanism of connexin-mediated growth suppression. *J. Biol. Chem.* **279,** 36943-36950.

Gellhaus, A., Dong, X., Propson, S., Maass, K., Klein-Hitpass, L., Kibschull, M., Traub, O., Willecke, K., Perbal, B., Lye, S. J. et al. (2004). Connexin43 interacts with NOV: A possible mechanism for negative regulation of cell growth in choriocarcinoma cells. *J. Biol. Chem.* **279,** 36931-36942.

Gershon, E., Plaks, V., Aharon, I., Galiani, D., Reizel, Y., Sela-Abramovich, S.,

Granot, I., Winterhager, E. and Dekel, N. (2008). Oocyte-directed depletion of connexin43 using the Cre-LoxP system leads to subfertility in female mice. *Dev. Biol.* **313**, 1-12.

Gittens, J. E., Barr, K. J., Vanderhyden, B. C. and Kidder, G. M. (2005). Interplay between paracrine signaling and gap junctional communication in ovarian follicles. *J. Cell. Sci.* **118,** 113-122.

Gittens, J. E., Mhawi, A. A., Lidington, D., Ouellette, Y. and Kidder, G. M. (2003). Functional analysis of gap junctions in ovarian granulosa cells: Distinct role for connexin43 in early stages of folliculogenesis. *Am. J. Physiol. Cell. Physiol.* **284,** C880-7.

Granot, I. and Dekel, N. (2002). The ovarian gap junction protein connexin43: Regulation by gonadotropins. *Trends Endocrinol. Metab.* **13,** 310-313.

Jiang, J. X. and Gu, S. (2005). Gap junction- and hemichannel-independent actions of connexins. *Biochim. Biophys. Acta* **1711,** 208-214.

Juneja, S. C., Barr, K. J., Enders, G. C. and Kidder, G. M. (1999). Defects in the germ line and gonads of mice lacking connexin43. *Biol. Reprod.* **60,** 1263-1270.

Kalcheva, N., Qu, J., Sandeep, N., Garcia, L., Zhang, J., Wang, Z., Lampe, P. D., Suadicani, S. O., Spray, D. C. and Fishman, G. I. (2007). Gap junction remodeling and cardiac arrhythmogenesis in a murine model of oculodentodigital dysplasia. *Proc. Natl. Acad. Sci. U. S. A.* **104,** 20512-20516.

Kidder, G. M. (2005). Roles of gap junctions in ovarian folliculogenesis: Implications for female infertility. In *Gap Junctions in Development and Disease* (ed. E. Winterhager), pp. 223-237: Springer-Verlag Berlin Heidelberg.

Laird, D. W. (2006). Life cycle of connexins in health and disease. *Biochem. J.* **394,** 527-543.

Langlois, S., Cowan, K. N., Shao, Q., Cowan, B. J. and Laird, D. W. (2008). Caveolin-1 and -2 interact with connexin43 and regulate gap junctional intercellular communication in keratinocytes. *Mol. Biol. Cell*. **19**, 912-928.

Langlois, S., Maher, A. C., Manias, J. L., Shao, Q., Kidder, G. M. and Laird, D. W. (2007). Connexin levels regulate keratinocyte differentiation in the epidermis. *J. Biol. Chem.* **282,** 30171-30180.

Loddenkemper, T., Grote, K., Evers, S., Oelerich, M. and Stogbauer, F. (2002). Neurological manifestations of the oculodentodigital dysplasia syndrome. *J. Neurol.* **249,** 584-595.

Manias, J. L., Plante, I., Gong, X. Q., Shao, Q., Churko, J., Bai, D. and Laird, D. W. (2008). Fate of connexin43 in cardiac tissue harbouring a disease-linked connexin43 mutant. *Cardiovasc. Res., in press* (PMID: 18678643)

McLachlan, E., Manias, J. L., Gong, X. Q., Lounsbury, C. S., Shao, Q., Bernier, S. M., Bai, D. and Laird, D. W. (2005). Functional characterization of oculodentodigital dysplasia-associated Cx43 mutants. *Cell. Commun. Adhes.* **12,** 279-292.

McLachlan, E., Plante, I., Shao, Q., Tong, D., Kidder, G. M., Bernier, S. M. and Laird, D. W. (2008). ODDD-linked Cx43 mutants reduce endogenous Cx43 expression and function in osteoblasts and inhibit late stage differentiation. *J. Bone Miner. Res.* **23**, 928-938.

Orisaka, M., Orisaka, S., Jiang, J. Y., Craig, J., Wang, Y., Kotsuji, F. and Tsang, B. K. (2006). Growth differentiation factor 9 is antiapoptotic during follicular development from preantral to early antral stage. *Mol. Endocrinol.* **20,** 2456-2468.

Paznekas, W. A., Boyadjiev, S. A., Shapiro, R. E., Daniels, O., Wollnik, B., Keegan, C. E., Innis, J. W., Dinulos, M. B., Christian, C., Hannibal, M. C. et al. (2003). Connexin 43 (GJA1) mutations cause the pleiotropic phenotype of oculodentodigital dysplasia. *Am. J. Hum. Genet.* **72,** 408-418.

Perez-Armendariz, E. M., Saez, J. C., Bravo-Moreno, J. F., Lopez-Olmos, V., Enders, G. C. and Villalpando, I. (2003). Connexin43 is expressed in mouse fetal ovary. *Anat. Rec. A. Discov. Mol. Cell. Evol. Biol.* **271,** 360-367.

Plante, I. and Laird, D. W. (2008). Decreased levels of connexin43 result in impaired development of the mammary gland in a mouse model of oculodentodigital dysplasia. *Dev. Biol.* **318,** 312-322.

Reaume, A. G., de Sousa, P. A., Kulkarni, S., Langille, B. L., Zhu, D., Davies, T. C., Juneja, S. C., Kidder, G. M. and Rossant, J. (1995). Cardiac malformation in neonatal mice lacking connexin43. *Science* **267,** 1831-1834.

Roscoe, W., Veitch, G. I., Gong, X. Q., Pellegrino, E., Bai, D., McLachlan, E., Shao, Q., Kidder, G. M. and Laird, D. W. (2005). Oculodentodigital dysplasia-causing connexin43 mutants are non-functional and exhibit dominant effects on wild-type connexin43. *J. Biol. Chem.* **280,** 11458-11466.

Shibayama, J., Paznekas, W., Seki, A., Taffet, S., Jabs, E. W., Delmar, M. and Musa, H. (2005). Functional characterization of connexin43 mutations found in patients with oculodentodigital dysplasia. *Circ. Res.* **96,** e83-e91.

Tong, D., Gittens, J. E., Kidder, G. M. and Bai, D. (2006). Patch-clamp study reveals that the importance of connexin43-mediated gap junctional communication for ovarian folliculogenesis is strain specific in the mouse. *Am. J. Physiol. Cell. Physiol.* **290,** C290-C297.

Vasconcellos, J. P., Melo, M. B., Schimiti, R. B., Bressanim, N. C., Costa, F. F. and Costa, V. P. (2005). A novel mutation in the *GJA1* gene in a family with oculodentodigital dysplasia. *Arch. Ophthalmol.* **123,** 1422-1426.

Veitch, G. I., Gittens, J. E., Shao, Q., Laird, D. W. and Kidder, G. M. (2004). Selective assembly of connexin37 into heterocellular gap junctions at the oocyte/granulosa cell interface. *J. Cell. Sci.* **117,** 2699-2707.

Wang, H. X., Tong, D., El-Gehani, F., Tekpetey, F. R. and Kidder, G. M. (2008). Connexin expression and gap junctional coupling in human cumulus cells: Contribution to embryo quality. *J. Cell. Mol. Med.*, in press (PMID: 18505471)

Figure legends

Fig. 1. Female *Gja1*^{Jrt}/+ mice have reduced fertility. A) After mating with wild-type males, the pregnancy rate of female *Gja1*^{Jrt}/+ mice was much lower than that of their wild-type littermates. B) Litters resulting from mating between *Gja1*^{Jrt}/+ females and wild-type males were significantly smaller ($P < 0.001$) compared with those from mating between wild-type females and wild-type males, and between wild-type females and *Gja1*^{Jrt}/+ males. C) The loss of pups was significantly higher ($P < 0.001$) when *Gja1*^{Jrt}/+ females were mated with wild-type males, compared with wild-type females with wild-type males and wild-type females with *Gja1*^{Jrt}/+ males. There was no significant difference between the latter two groups ($P > 0.05$).

Fig. 2. *Gja1*^{Jrt}/+ ovaries contain normal numbers of germ cells. A) Ovaries from postnatal day 1 wild-type (top row) and *Gja1*^{Jrt}/+ (bottom row) females were co-immunolabeled for the germ cell marker GCNA (red) and Cx43 (green). Nuclei were stained with Hoechst (blue). The higher magnification picture (far right column) shows that the gap junction "plaques" (white arrows) formed in wild-type ovaries are rarely present in *Gja1*^{Jrt}/+ ovaries. Scale bar = 20 μm. B) Quantification of germ cell numbers per ovary from wild-type and *Gja1*^{Jrt}/+ females ($P = 0.71$).

Fig. 3. *Gja1*^{Jrt}/+ ovaries contain fewer pre-ovulatory follicles and have reduced response to gonadotropins. A) Distribution of follicles at different developmental stages in the wild-type and *Gja1*^{Jrt}/+ ovaries ($P > 0.05$). B) Quantification of early and late antral follicles in the wild-type and *Gja1*^{Jrt}/+ ovaries during proestrus (wild-type vs.

Gja1^{Jrt}/+, P > 0.05 for early antral, P < 0.05 for late antral). C) Quantification of COCs collected from oviducts of wild-type and *Gja1*^{Jrt}/+ mice after priming with eCG and hCG (P < 0.01). D) Percentage of oocytes that cleaved to the 2-cell stage after in vitro fertilization (P > 0.05).

Fig. 4. Aberrant phosphorylation and trafficking of Cx43 in *Gja1*^{Jrt}/+ granulosa cells. A) Western blot analysis demonstrated that the abundance of total Cx43 protein in ovaries from *Gja1*^{Jrt}/+ mice is not significantly different (P > 0.05) from wild-type littermates. However, the phosphorylated P1 and P2 forms of Cx43 are significantly reduced in the mutant ovaries (P < 0.01). In contrast, the abundance of Cx43 in hearts from *Gja1*^{Jrt}/+ mice is significantly lower than wild-type in terms of both total Cx43 and its phosphorylated forms (P < 0.001). Cx43 abundance is expressed relative to GAPDH. B) Representative micrographs showing ovaries from 6-8 week old wild-type (top row) and *Gja1*^{Jrt}/+ (bottom row) females immunolabeled for Cx43 (green). Nuclei were stained with Hoechst (blue). The magnified micrograph (far right column) shows that there are numerous gap junction "plaques" in wild-type ovarian follicles, whereas very few similar structures are seen in *Gja1*^{Jrt}/+ follicles. Scale bar = 20 μm. C) Primary granulosa cells isolated from ovaries of wild-type (top row) or *Gja1*^{Jrt}/+ (bottom row) mice were co-immunolabeled for Cx43 (green) and the Golgi marker GM130 (red). Nuclei were stained with Hoechst (blue). The merged image shows co-localization (yellow within white circles) in *Gja1*^{Jrt}/+ cells. White arrows indicate the gap junction plaques formed between neighboring cells in both cell populations.

Fig. 5. Reduced proliferation of granulosa cells. A) Data are expressed as the percentage of granulosa cells that incorporated BrdU relative to the total number of cells in a field of view, counted after Hoechst staining ($P < 0.05$). B) Primary cultured granulosa cells were immunolabeled for PCNA and the signal intensity was quantified and normalized to one of the wild-type granulosa cell readings from the same experiment ($P < 0.01$).

Fig. 6. Elevated apoptosis in *Gja1*^{Jrt}/+ antral follicles indicated by TUNEL assay. A) Representative pictures showing apoptotic cells in the ovaries from 6-8 week old wild-type (left column) and *Gja1*^{Jrt}/+ (middle column) females. Right column is the positive control pre-treated with DNase. Fluorescent images are shown in the top row while corresponding phase contrast pictures are merged in the bottom row to show the tissue structure. White arrows indicate antral follicles. Scale bar = 100 μm. B) The fluorescence intensities in the antral follicles were quantified relative to follicle area and found to differ significantly between genotypes ($P < 0.05$).

Fig. 7. Unchanged oocyte-granulosa cell coupling and GDF9 expression in *Gja1*^{Jrt}/+ ovaries. A) Microinjection of Lucifer yellow into cumulus-enclosed oocytes demonstrated that injected dye can pass readily from the oocyte to surrounding cumulus cells in both wild-type and *Gja1*^{Jrt}/+ follicles. Scale bar = 100 μm. B) Western blot analysis demonstrated that the abundance of GDF9 in ovaries from *Gja1*^{Jrt}/+ mice is not significantly different from wild-type littermates ($P > 0.05$). GDF9 abundance is expressed relative to GAPDH.

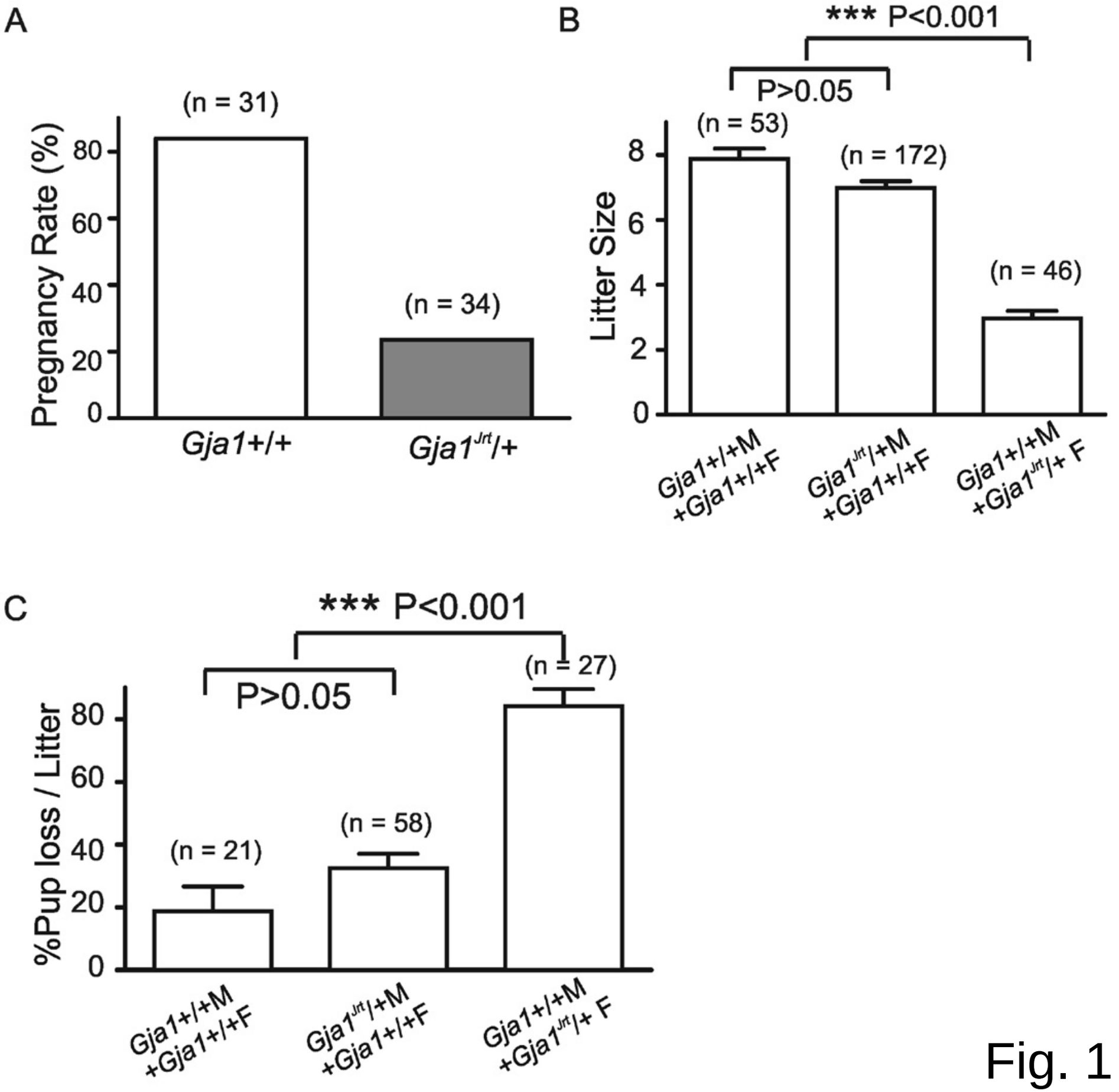
A
Pregnancy Rate (%)
0
20
40
60
80
(n = 31)
(n = 34)
Gja1+/+
Gja1Jrt/+
B
*** P<0.001
P>0.05
Litter Size
0
2
4
6
8
(n = 53)
(n = 172)
(n = 46)
Gja1+/+M
+Gja1+/+F
Gja1Jrt/+M
+Gja1+/+F
Gja1+/+M
+Gja1Jrt/+ F
C
*** P<0.001
P>0.05
%Pup loss / Litter
0
20
40
60
80
(n = 21)
(n = 58)
(n = 27)
Gja1+/+M
+Gja1+/+F
Gja1Jrt/+M
+Gja1+/+F
Gja1+/+M
+Gja1Jrt/+ F

Fig. 1

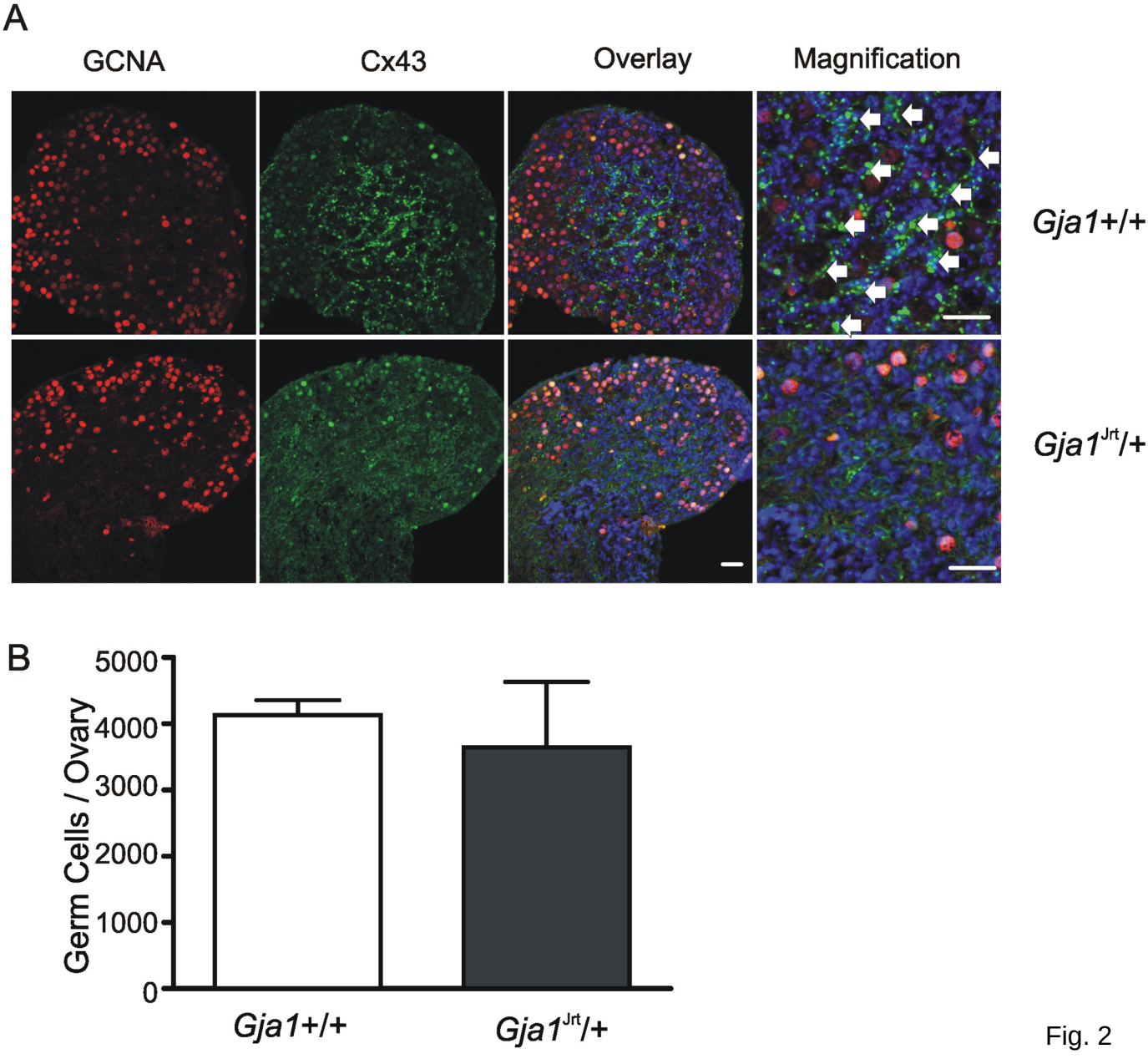
A
GCNA
Cx43
Overlay
Magnification
Gja1+/+
Gja1Jrt/+
B
Germ Cells / Ovary
5000
4000
3000
2000
1000
0
Gja1+/+
Gja1Jrt/+

Fig. 2

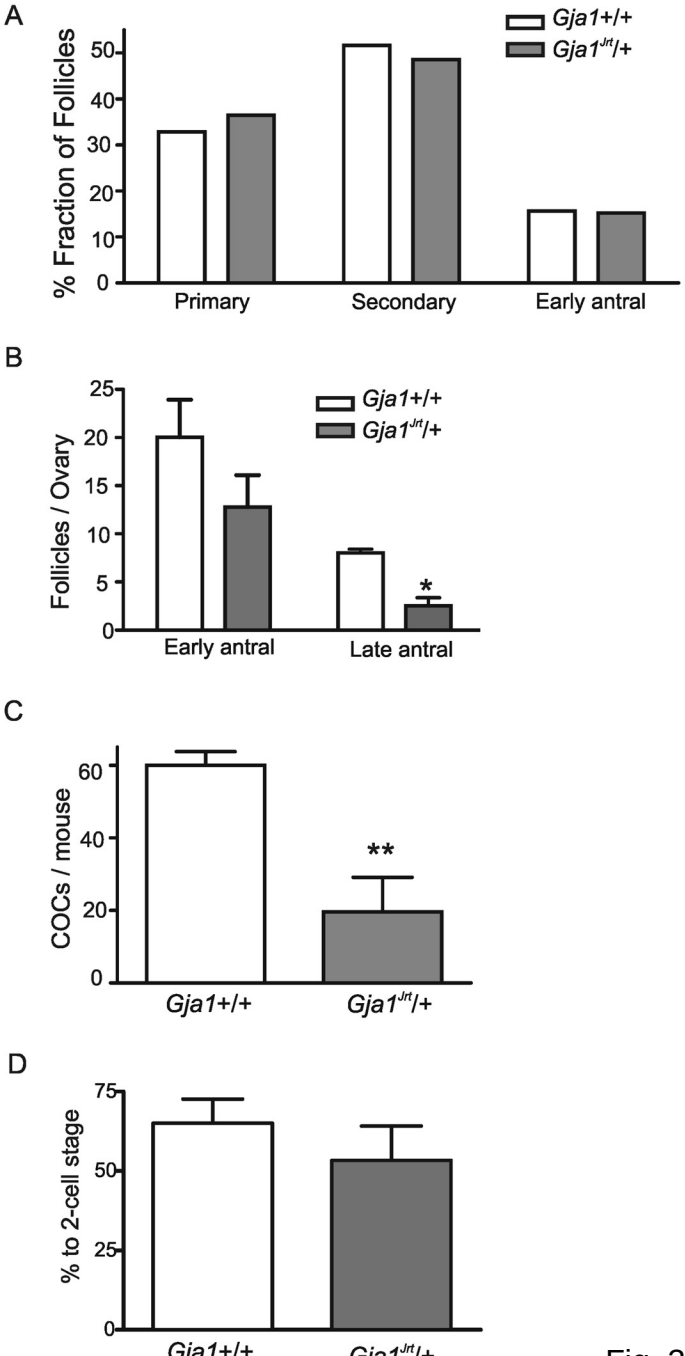
A
Gja1+/+
Gja1Jrt/+
% Fraction of Follicles
50
40
30
20
10
0
Primary
Secondary
Early antral
B
Gja1+/+
Gja1Jrt/+
Follicles / Ovary
25
20
15
10
5
0
*
Early antral
Late antral
C
COCs / mouse
60
40
20
0
**
Gja1+/+
Gja1Jrt/+
D
% to 2-cell stage
75
50
25
0
Gja1+/+
Gja1Jrt/+

Fig. 3

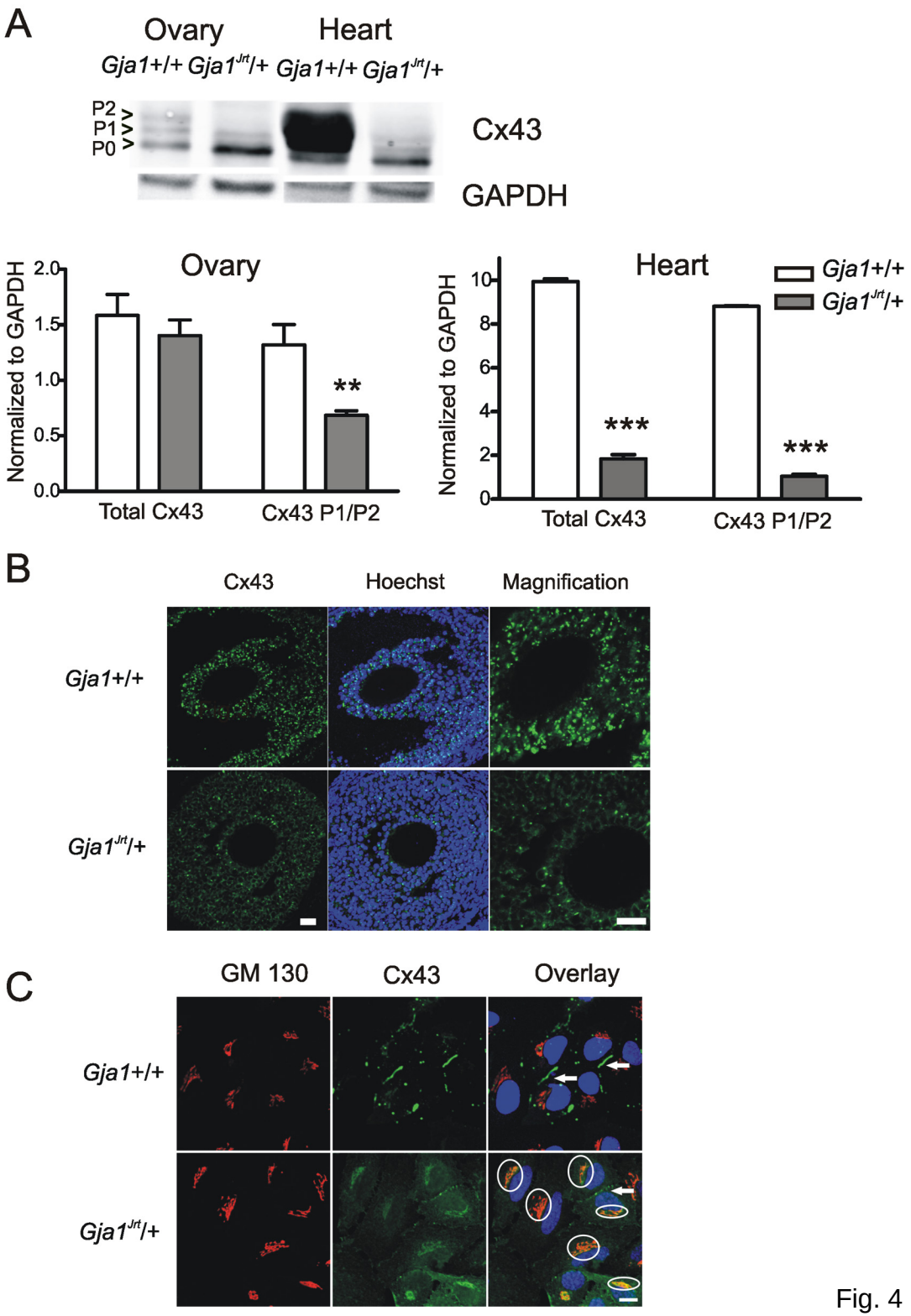
A
Ovary
Heart
Gja1+/+ Gja1Jrt/+ Gja1+/+ Gja1Jrt/+
P2
P1
P0
Cx43
GAPDH
Ovary
Normalized to GAPDH
2.0
1.5
1.0
0.5
0.0
**
Total Cx43
Cx43 P1/P2
Heart
Gja1+/+
Gja1Jrt/+
Normalized to GAPDH
10
8
6
4
2
0
***
***
Total Cx43
Cx43 P1/P2
B
Cx43
Hoechst
Magnification
Gja1+/+
Gja1Jrt/+
C
GM 130
Cx43
Overlay
Gja1+/+
Gja1Jrt/+

Fig. 4

Fig. 5

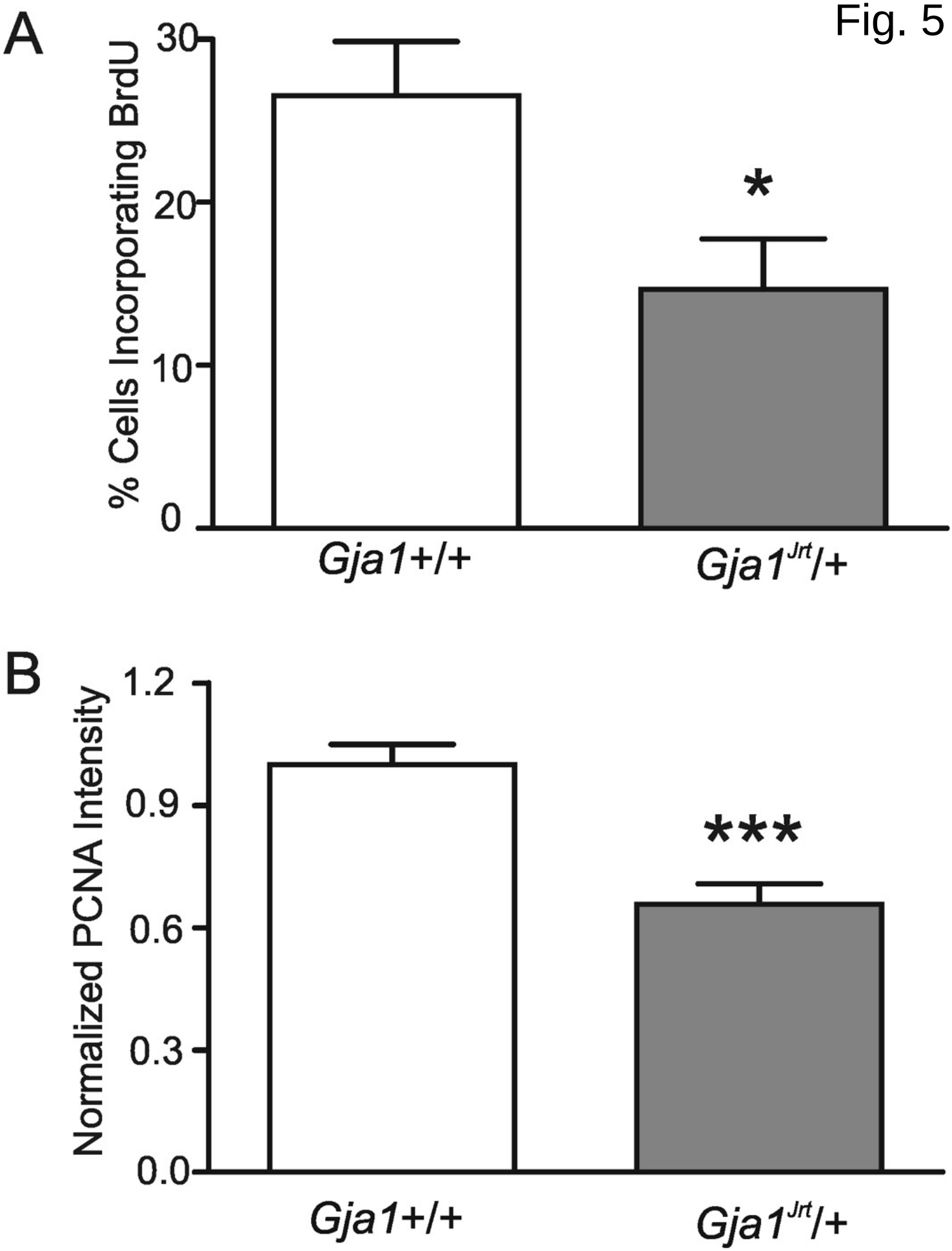
A
% Cells Incorporating BrdU
30
20
10
0
*
Gja1+/+
Gja1Jrt/+
B
Normalized PCNA Intensity
1.2
0.9
0.6
0.3
0.0
***
Gja1+/+
Gja1Jrt/+

A

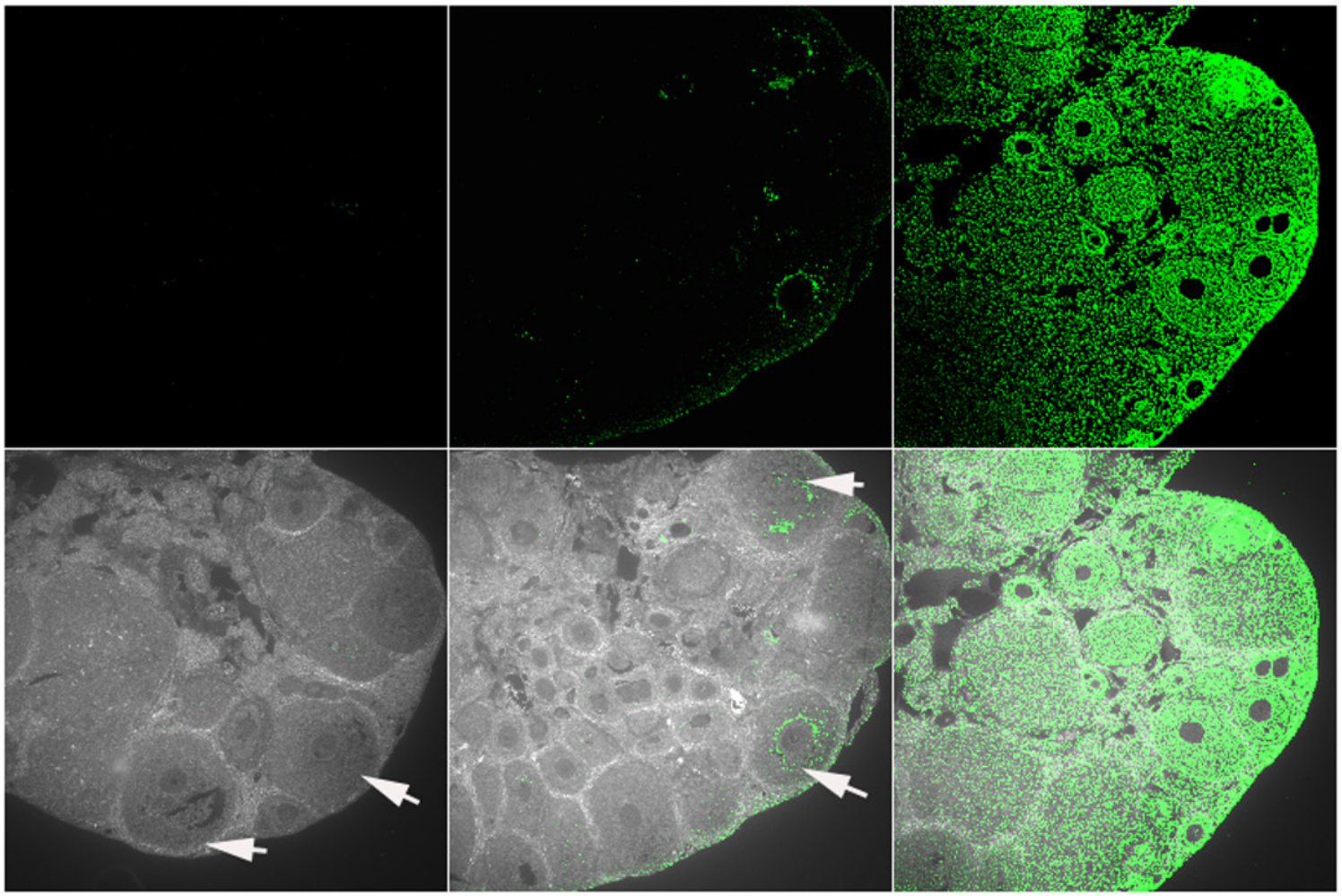

B

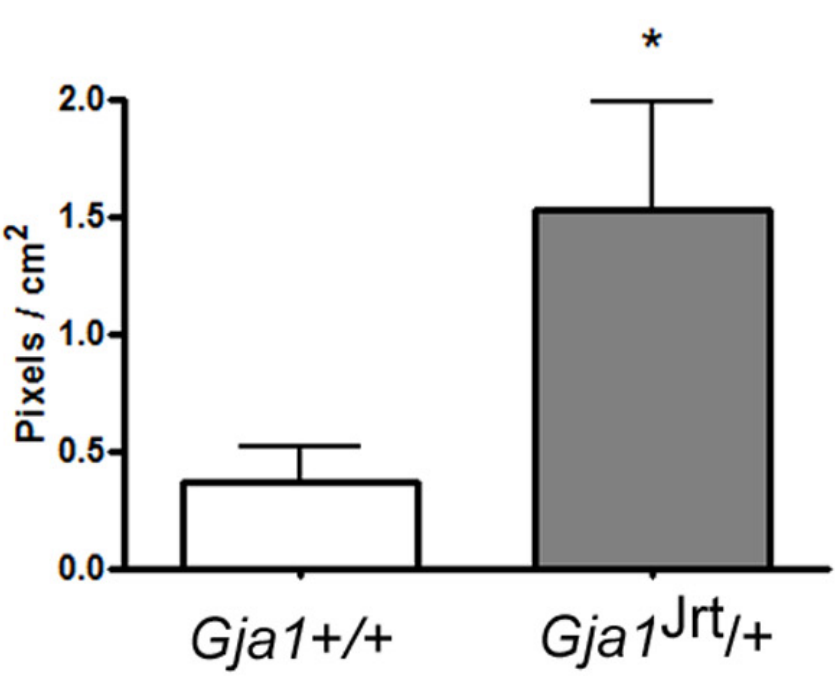

Fig. 6

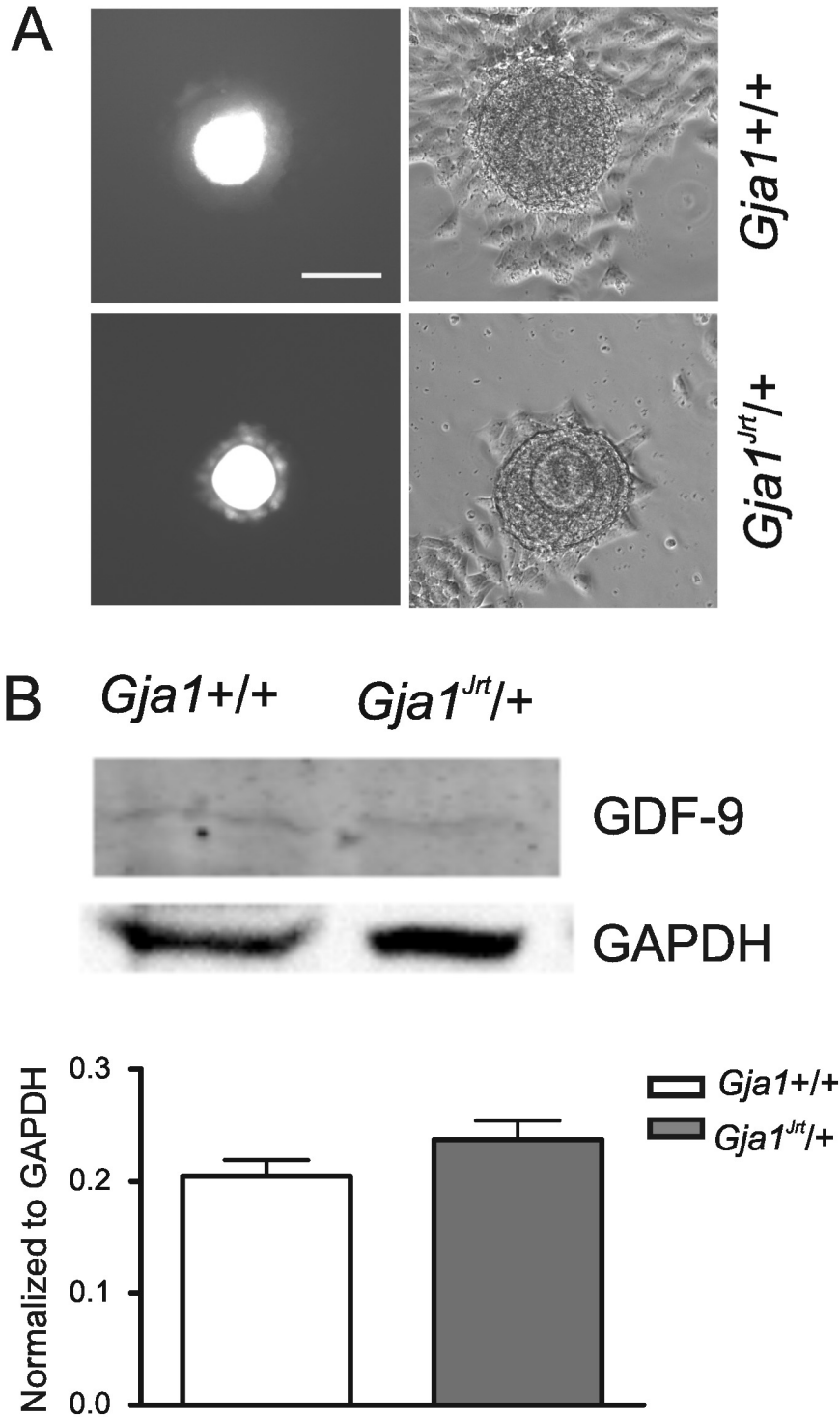
A
Gja1+/+
Gja1Jrt/+
B
Gja1+/+
Gja1Jrt/+
GDF-9
GAPDH
Normalized to GAPDH
0.3
0.2
0.1
0.0
Gja1+/+
Gja1Jrt/+

Fig. 7